

Simple Solid-State Chemical Synthesis of ZnSnO₃ Nanocubes and Their Application as Gas Sensors

Yali Cao,^[a,b] Dianzeng Jia,^{*[a,b]} Jie Zhou,^[a] and Ying Sun^[a]

Keywords: Oxides / Nanostructures / Solid-phase synthesis / Sensors

New ZnSnO₃ nanocubes were synthesized by a simple PEG-induced solid-state chemical reaction between metal salts and NaOH; this process is cheap and proceeds in a relatively simple manner. The uniform cubic nanostructures were fully characterized. The gas-sensing properties of ZnSnO₃ were investigated in detail. The results indicated that ZnSnO₃ nanocubes possess good gas-sensing properties for ethanol and methanal; thus, these nanocubes show excellent poten-

tial for ethanol and methanal sensors. This strategy is expected to be extendable to other composite nanomaterials with special morphologies in solid-state routes by selecting an appropriate reaction and its corresponding inducing reagent.

(© Wiley-VCH Verlag GmbH & Co. KGaA, 69451 Weinheim, Germany, 2009)

Introduction

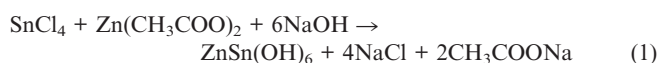
Direct fabrication of nanostructures with controlled morphologies, orientations, and dimensionalities has attracted much attention since it is was learned that the physical and chemical properties of materials can be strongly influenced by their sizes and shapes.^[1–7] The study of composite metal oxides (CMOs) is always interesting to investigate because of their superiority over single metal oxides in many cases,^[8,9] for example, as gas-sensor materials. Reported results show good sensitivity over simple oxides and can improve the selectivity of sensing materials to different reducing and oxidizing gases.^[10–13]

Current studies on CMO materials have been focused on zero-dimensional microparticles or nanoparticles, and little work has been devoted to 1D nanomaterials, which can be synthesized by various well-established techniques, including a chemical solution route, template synthesis, chemical vapor deposition, thermal evaporation, and a template-induced, citrate-based, sol–gel process.^[14–20] To date, we have found nothing in the literature on the synthesis of cubic CMO nanomaterials. Furthermore, reported methods suffer from inherent drawbacks, such as the involvement of complex processes, rigorous conditions, or long reaction times. The development of a facile controllable synthesis method for cubic CMO nanostructures was deemed very important to be able to explore their novel properties and to examine potential applications of CMOs.

Herein we report a simple solid-state chemical synthesis of new ZnSnO₃ nanocubes. The use of solid-state chemical reaction methods for growing nanomaterials including nanoparticles, nanorods, nanotubes, and hollow nanostructures has received much attention, as these processes tend to be simple, cheap, high yielding, and only require mild reaction conditions.^[21–26] Here, the method was further developed to synthesize new cubic CMO nanomaterials by using polyethylene glycol (PEG) as an inducing reagent to change the growth microenvironment of the solid-state chemical reaction. To the best of our knowledge, there are no reports on the preparation of cubic CMO nanomaterials through the use of solid-state chemical methods. In addition, the gas-sensing characteristics of the as-prepared ZnSnO₃ nanocubes were performed to explore their possible applications.

Results and Discussion

We fabricated ZnSnO₃ nanocubes after annealing the precursor, which was synthesized by solid-state chemical reaction between metal salts and alkali at room temperature. The reaction process can be described by Equations (1) and (2).



We first present the structural characteristics of the ZnSnO₃ nanocubes. Figure 1 shows the X-ray diffraction (XRD) patterns of the final product and precursor prepared by a solid-state chemical reaction. The diffraction

[a] Institute of Applied Chemistry, Xinjiang University, Urumqi, Xinjiang 830046, P. R. China
Fax: +86-991-8580032
E-mail: jdz@xju.edu.cn

[b] School of Science, Xi'an Jiaotong University, Xi'an, Shanxi 710049, P. R. China

peaks of the precursor shown in Figure 1a are quite similar to those of standard $\text{ZnSn}(\text{OH})_6$, which can be indexed as $\text{ZnSn}(\text{OH})_6$ with cubic phase (JCPDF Card file NO.20-1455). No characteristic peaks of impurities, such as reactants and other byproducts, were observed in the precursor. From the thermogravimetric analysis (TGA) curves of the precursor (Figure 2a), we can observe a weight loss of 18.53%, which is close to the theoretical weight loss value (18.87%) for decomposition of the precursor from $\text{ZnSn}(\text{OH})_6$ to ZnSnO_3 . So, we can deduce that the precursor is $\text{ZnSn}(\text{OH})_6$ and select 500 °C as the annealing temperature to produce the final product. The diffraction patterns of the final product are similar to hexagonal ZnSnO_3 (JCPDF Card file NO.28-1486), which is displayed in Figure 1b. The relative intensity of the diffraction peaks has some variation owing to the different crystal structure and the peculiar cubic morphology of the final product. A weight loss of less than 3% was observed for the final product, which can be attributed to the dehydration of the physically absorbed water molecules (Figure 2b). The energy-dispersive X-ray spectroscopy (EDS) result of the final product revealed the presence of Zn, Sn, and O with an atomic ratio of 1.08:1:3.14 (Figure 2c). These results indicate that the $\text{ZnSn}(\text{OH})_6$ precursor has entirely decomposed into the final ZnSnO_3 product after annealing at 500 °C.

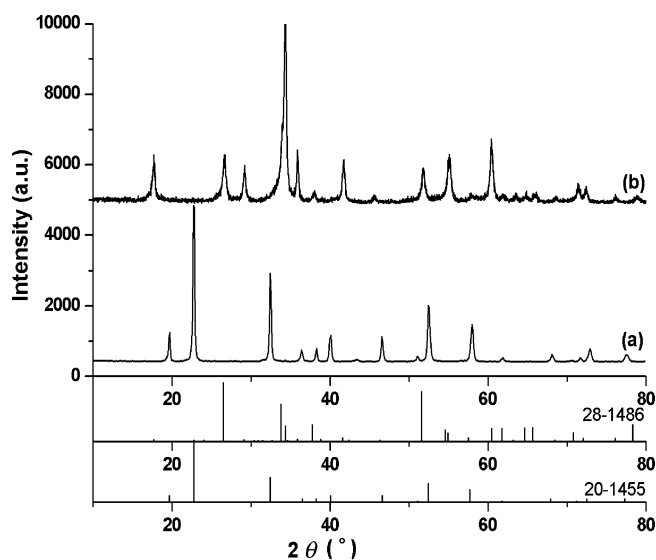


Figure 1. XRD patterns of (a) the precursor and (b) the final product.

The morphological characteristics of the product were performed by scanning electron microscopy (SEM) and transmission electron microscopy (TEM). Figure 3a–d shows the morphologies of the precursor and final product. A low-magnification SEM image shows that the dominant components of the precursor and final product are nanocubes with a uniform size distribution. Typical TEM images of the final product provide evidence that the ZnSnO_3 nanocubes have a perfect cubic shape. The edge of the cubes is 60–110 nm. Additional structural characterization of the ZnSnO_3 nanocubes was carried out by selected area elec-

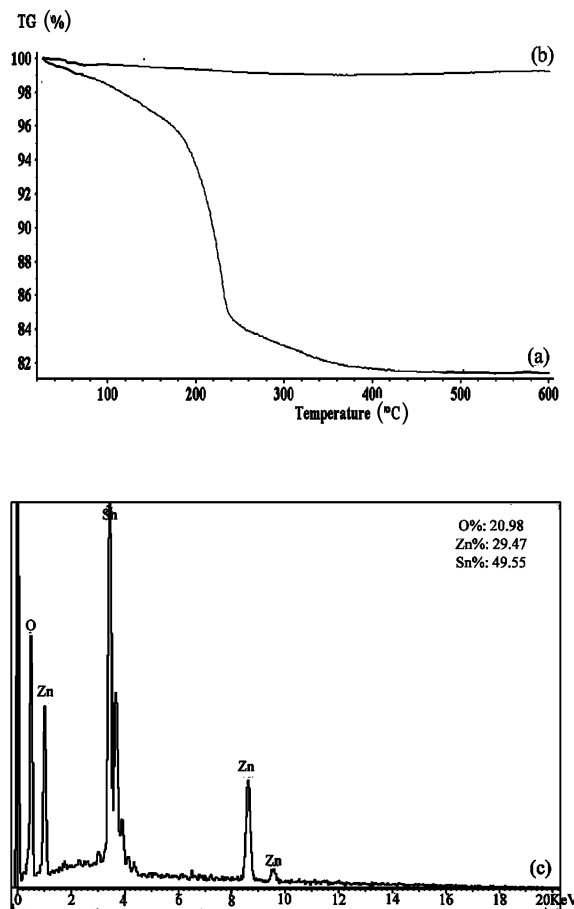


Figure 2. TG curves of (a) the precursor and (b) the final product; (c) EDS patterns of the final product.

tron diffraction (SAED) and high-resolution transmission electron microscopy (HRTEM). A corresponding SAED pattern of the nanocubes is shown in Figure 3e and suggests that the product has good crystallinity. Figure 3f shows a typical HRTEM image of an individual nanocube. The image shows the clear fringes with a latter spacing of about 0.263 nm, corresponding to the (110) lattice planes of hexagonal ZnSnO_3 .

Recently, the introduction of the solid-state chemical reaction technique has provided a relatively simple and powerful method for controlling the size, shape, and surface texture of nanomaterials.^[21–26] In this study, the special nanocubes were obtained by a solid-state chemical reaction in the presence of PEG 400. In order to understand the effect of the PEG 400 raw material on the microstructure of the product, ZnSnO_3 was also prepared by following the same procedure but without the addition of PEG 400. The results indicate that the nanocubes cannot be formed without the presence of PEG 400. Thus, the surfactant, PEG 400, plays an important role in the formation of the nanocubes. Here, PEG 400 was introduced into the solid-state reaction system and involved in the reaction process. In such solid-state reaction microenvironments, the product particles are encapsulated in the closed or half-closed shells

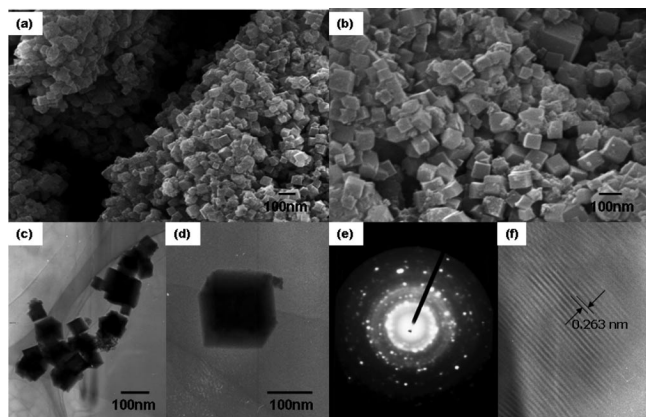


Figure 3. SEM images of (a) the precursor and (b) the final product; (c,d) TEM images of the final product; (e) SARD and (f) HRTEM images of the final product.

of the surfactant molecules, which blocks up the continued growth and agglomeration of product particles. Simultaneously, PEG acts as an inducing reagent to influence the growth of the product. Then, the precursor is assembled into nanocubes as a result of the interaction between two metal ions and a negative ion as well as its personal crystal growth propensity under the inducing role of PEG. The exact mechanism is still under investigation. After the annealing process, ZnSn(OH)_6 decomposed into ZnSnO_3 , but its cubic shape remained. The formation of CMO nanomaterials with rod-, plate-, and flower-like morphologies are carried out using such solid-state routes by selecting an appropriate reaction and its corresponding inducing reagent at the moment. This strategy is expected to be applicable to the growth of composite sulfides with special morphologies.

Methanal and xylene are well-known toxic chemicals, and they are hazardous to our health and to the environment. Ammonia is a corrosive liquid that can give off a strongly irritating smell. Flammable and explosive gases, such as liquefied petroleum gas, gasoline, and H_2 , can be harmful and dangerous. It is very necessary to effectively detect and monitor them by using a suitable technique. Therefore, the development of novel sensing materials for gases is of importance. The gas-sensing properties of the as-synthesized ZnSnO_3 nanocubes were investigated in this study.

Eight gases were selected to test the gas-sensing properties of the ZnSnO_3 nanocubes. Figure 4 shows the relationship between the working temperature and the sensitivity of the sensor to various gases, including ethanol ($\text{C}_2\text{H}_5\text{OH}$), methanal (HCHO), 93[#] gasoline, xylene [$\text{C}_6\text{H}_4(\text{CH}_3)_2$], ethoxyethane [$(\text{CH}_3\text{CH}_2)_2\text{O}$], liquefied petroleum gas (LPG), hydrogen (H_2), and ammonia (NH_3) at a concentration of 100 ppm. For target gases, which decrease the resistance of the gas sensors, the sensitivity of the sensors was determined as the $R_{\text{air}}/R_{\text{gas}}$ ratio, where R_{air} is the resistance of the sensors in air and R_{gas} is that in the gas tested. The sensitivity curves of the eight gases indicate that the ZnSnO_3 -nanocube-based sensors have good response properties. For ethanol and methanal, the ZnSnO_3 nanocubes

have high signal response. The response value can reach up to 34.2 and 18.8 for 100 ppm ethanol and methanal at a working temperature of about 300 and 332 °C, respectively. The response value of the as-synthesized ZnSnO_3 nanocubes was much better than that of the commercial ZnSnO_3 powder, which was 8.9 and 2.3. It is clear that the enhancement in gas sensitivity of the nanocubes can be attributed to the higher surface-to-volume ratio than that of the commercial powder.

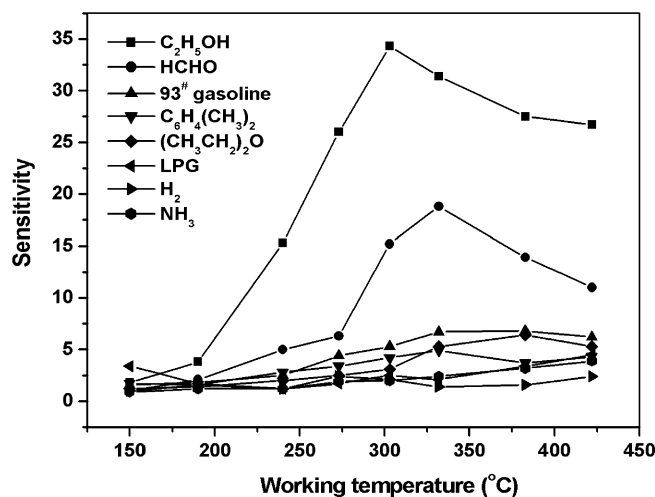


Figure 4. Relationship between working temperature and sensitivity of sensor to various gases at a concentration of 100 ppm.

The gas-sensing characteristics of the ZnSnO_3 nanocubes were also found to be remarkably stable and reproducible over 10 repeated test cycles. The response time is defined as the time required for the conductance to reach 90% of the equilibrium value after the test gas is injected. The response times to 100 ppm ethanol and methanal were about 4 and 7 s, respectively. The recovery time is the time necessary for the sensor to attain a conductance that is 10% higher than the original value in air after the test gas is removed. The recovery times to 100 ppm ethanol and methanal were 11 and 16 s, respectively. The response and recovery properties were much better than the commercial powder, which had response and recovery times of 26 and 45 s, respectively. These results are in accordance with the practical use required for a gas sensor, which should provide not only high response and good selectivity but also rapid response to and recovery of the target gas.

The variation in sensitivity at different concentrations of ethanol and methanal is shown in Figure 5. These measurements were performed by injecting various amounts of ethanol and methanal into the sealed chamber at an operating temperature of 300 and 332 °C. The sensor response increased with an increase in ethanol and methanal gas concentration. When the ethanol concentration was in the range 10–100 ppm, the sensitivity showed relatively good linearity with the gas concentration. Specifically, the ZnSnO_3 nanocubes were found to exhibit excellent ethanol gas responses even at very low concentrations, so it can be expected to serve as an excellent functional component in

ethanol gas sensors. In addition to that, the special cubic ZnSnO_3 nanomaterials can be also designed to detect noxious pollutants of methanal at relatively low temperatures.

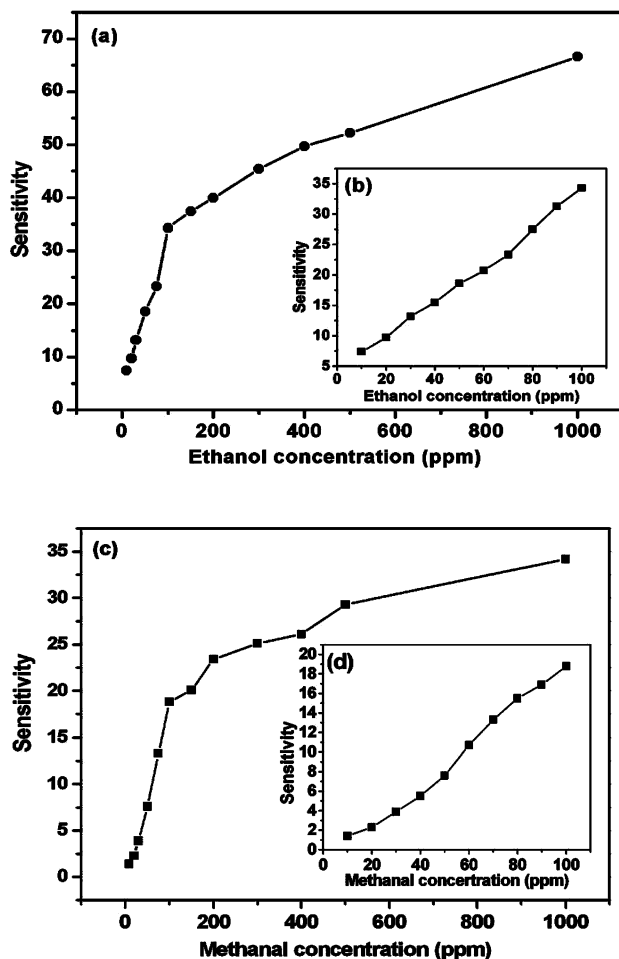


Figure 5. Relationship between sensitivity of sensor and gas concentration: (a,b) ethanol, (c,d) methanal.

Conclusions

In summary, new ZnSnO_3 nanocubes were synthesized by using a solid-state chemical reaction technique. The gas-sensing measurement results indicate that a sensor based on the ZnSnO_3 nanocubes shows high response and good selectivity and also rapid response and recovery to ethanol and methanal. The excellent sensing properties of the ZnSnO_3 nanocubes may allow these materials to be used in the development of ethanol and methanal gas-sensing devices. This strategy is expected to be applicable to the growth of other composites with special morphologies.

Experimental Section

General: All reagents were analytically pure, purchased from commercial sources, and used without further purification. XRD were performed with a MAC Science MXP18AHF X-ray diffractometer

equipped with graphite-monochromated $\text{Cu-K}\alpha$ radiation ($\lambda = 1.54056 \text{ \AA}$). TGA were obtained under an atmosphere of nitrogen with a NETZSCH STA 449C thermal analyzer. EDS was examined with an Oxford 2000 energy disperse X-ray spectroscopy. TEM images were made with a Hitachi H-600 transmission electron microscope. SEM images were performed with an LEO1430VP scanning electron microscope. The SAED patterns and HRTEM images were observed with a JEOL-2010 high-resolution transmission electron microscope. The gas-sensing properties were measured in a glass test chamber by using a HW-30A gas-sensing static measuring system (Hanwei Electronics Co. Ltd., P.R. China).

Typical Procedure for the Synthesis of ZnSnO_3 Nanocubes: Solid $\text{SnCl}_4 \cdot 5\text{H}_2\text{O}$ and $\text{Zn}(\text{CH}_3\text{COO})_2 \cdot 2\text{H}_2\text{O}$ in a mole ratio of 1:1 were ground for several minutes in an agate mortar and then mixed and blended with an adequate amount of PEG 400. After the mixture was ground, solid NaOH power (with a mol ratio of 1:3 between $\text{SnCl}_4 \cdot 5\text{H}_2\text{O}$ and NaOH) was mixed and ground. After a few minutes of grinding, water vapor started to rise from the mixture, signaling the start of the reaction. The mixture was continually ground for another 30 min, and the byproduct salt and PEG were washed away with distilled water and alcohol in an ultrasonic bath and dried in air to obtain the precursor. Then, the white precursor powder was calcined at 500°C for 3 h under an atmosphere of nitrogen to obtain the final product powder.

Preparation of the Gas Sensors: An appropriate quantity of terpinol was added to the as-prepared ZnSnO_3 nanocubes, and the mixture was ground in an agate mortar to form a paste. The mixture was then coated onto the surface of ceramic tubes with two Pt electrodes to obtain thick films. After annealing at 500°C for 1 h, a resistance heater was then inserted into the ceramic tubes to control the working temperature of the sensors. Side-heating-type devices were aged at 350°C for 7 d to improve the stability before testing.

Acknowledgments

This work was financially supported by the National Science Foundation of Xinjiang Province (No. 200721102), the National Science Foundation of China (Nos. 20661003 and 20861008), and the Scientific Research Foundation in Xinjiang Educational Institutions (XJEDU2007S06). The authors wish to thank the referees for their careful reading of the manuscript and helpful suggestions.

- [1] Y. N. Xia, P. D. Yang, Y. G. Sun, Y. Y. Wu, B. Mayers, B. Gates, Y. D. Yin, F. Kim, H. Q. Yan, *Adv. Mater.* **2003**, *15*, 353–389.
- [2] A. Kolmakov, D. O. Klenov, Y. Lilach, S. Stemmer, M. Moskovits, *Nano Lett.* **2005**, *5*, 667–673.
- [3] J. Chen, L. N. Xu, W. Y. Li, X. L. Gou, *Adv. Mater.* **2005**, *17*, 582–586.
- [4] C. S. Rout, S. H. Krishna, S. R. C. Vivekchand, A. Govindaraj, C. N. R. Rao, *Chem. Phys. Lett.* **2006**, *418*, 586–590.
- [5] W. W. Wang, Y. J. Zhu, L. X. Yang, *Adv. Funct. Mater.* **2007**, *17*, 59–64.
- [6] Z. H. Dai, J. Zhang, J. C. Bao, X. H. Huang, X. Y. Mo, *J. Mater. Chem.* **2007**, *17*, 1087–1093.
- [7] X. L. Gou, G. X. Wang, X. Y. Kong, D. Wexler, J. Horvat, J. Yang, J. Park, *Chem. Eur. J.* **2008**, *14*, 5996–6002.
- [8] R. L. D. Whitby, K. S. Brigatti, I. A. Kinloch, D. P. Randall, T. Maekaw, *Chem. Commun.* **2004**, 2396–2397.
- [9] T. Zhang, C. G. Jin, T. Qian, X. L. Lu, J. M. Bai, X. G. Li, *J. Mater. Chem.* **2004**, *14*, 2787–2789.
- [10] X. F. Chu, D. L. Jiang, Y. Guo, C. M. Zheng, *Sens. Actuators B* **2006**, *120*, 177–181.

- [11] J. Q. Xu, X. H. Jia, X. D. Lou, J. N. Shen, *Solid-State Electron.* **2006**, *50*, 504–507.
- [12] X. F. Chu, D. L. Jiang, C. M. Zheng, *Sens. Actuators B* **2007**, *123*, 793–797.
- [13] J. Wang, Y. J. Wu, Y. J. Zhu, P. Q. Wang, *Mater. Lett.* **2007**, *61*, 1522–1525.
- [14] S. H. Yu, B. Liu, M. S. Mo, J. H. Huang, X. M. Liu, Y. T. Qian, *Adv. Funct. Mater.* **2003**, *13*, 638–647.
- [15] J. Wang, Q. W. Chen, B. Y. Hou, Z. M. Peng, *Eur. J. Inorg. Chem.* **2004**, 1165–1168.
- [16] Z. T. Zhang, A. J. Rondinone, J. X. Ma, J. Shen, D. Dai, *Adv. Mater.* **2005**, *17*, 1415–1419.
- [17] J. H. Lee, H. J. Park, K. Yoo, B. W. Kim, J. C. Lee, S. Park, *J. Eur. Ceram. Soc.* **2007**, *27*, 965–968.
- [18] A. V. Ghule, K. Ghule, S. H. Tzing, Y. C. Ling, *Eur. J. Inorg. Chem.* **2007**, 3342–3349.
- [19] C. W. Na, D. S. Han, J. H. Park, Y. H. Jo, M. H. Jung, *Chem. Commun.* **2006**, 2251–2253.
- [20] Z. Yang, Y. Huang, B. Dong, H. L. Li, S. Q. Shi, *J. Solid State Chem.* **2006**, *179*, 3324–3329.
- [21] X. R. Ye, D. Z. Jia, J. Q. Yu, X. Q. Xin, Z. L. Xue, *Adv. Mater.* **1999**, *11*, 941–943.
- [22] F. Li, H. G. Zheng, D. Z. Jia, X. Q. Xin, Z. L. Xue, *Mater. Lett.* **2002**, *53*, 282–286.
- [23] T. Y. Zhou, X. Q. Xin, *Nanotechnology* **2004**, *15*, 534–536.
- [24] Y. L. Cao, L. Liu, D. Z. Jia, X. Q. Xin, *Chin. J. Chem.* **2005**, *23*, 539–542.
- [25] Z. P. Sun, L. Liu, L. Zhang, D. Z. Jia, *Nanotechnology* **2006**, *17*, 2266–2270.
- [26] R. Y. Wang, D. Z. Jia, L. Zhang, L. Liu, Z. P. Guo, B. Q. Li, J. X. Wang, *Adv. Funct. Mater.* **2006**, *16*, 687–692.

Received: February 11, 2009

Published Online: August 12, 2009